

Avoidance of Disruptions at High β_N in ASDEX Upgrade with Off-Axis ECRH

B. Esposito 1), G. Granucci 2), M. Maraschek 3), S. Nowak 2), A. Gude 3), V. Igochine 3), R. McDermott 3), E. Poli 3), J. Stober 3), W. Suttrop 3), W. Treutterer 3), H. Zohm 3), and ASDEX Upgrade 3) team

1) Associazione EURATOM-ENEA sulla Fusione, C.R. Frascati, Via E. Fermi 45, 00044 Frascati (Roma), Italy

2) Associazione EURATOM-ENEA sulla Fusione, IFP-CNR, Via R. Cozzi 53, 20125 Milano, Italy

3) Max-Planck-Institut für Plasmaphysik, EURATOM Association, Boltzmannstr. 2, 85748 Garching bei München, Germany

e-mail contact of main author: Basilio.Esposito@enea.it

Abstract. Experiments on disruption avoidance have been carried out in H-mode ASDEX Upgrade plasmas: the localized perpendicular injection of ECRH (1.5 MW $\sim 0.2 P_{tot}$) onto the $q=2$ resonant surface has led to the delay and/or complete avoidance of disruptions in a high β_N scenario ($I_p=1$ MA, $B_t=2.1$ T, $q_{95}\sim 3.6$, with NBI ~ 7.5 MW). In these discharges (at low q_{95} and low density) neoclassical tearing modes (NTMs) are excited: the growth and locking of the $m/n=2/1$ mode leads to the disruption. The scheme of the experiment is the same successfully applied in previous disruption avoidance experiments in FTU and ASDEX Upgrade. As soon as the disruption precursor signal (the locked mode detector and/or the loop voltage) reaches the preset threshold, the ECRH power is triggered by real time control. A poloidal scan in deposition location (ρ_{dep}) has been carried out by setting the poloidal launching mirrors at different angles in each discharge. The results depend on ρ_{dep} : complete disruption avoidance can be achieved when the power is injected close to or onto the 2/1 island. When ECRH is injected outside the island (either at radii inside or outside the $q=2$ surface), the discharge disrupts as in the reference case.

1. Introduction

The study of the control of disruptions in tokamak plasmas by means of electron cyclotron resonance heating (ECRH) has been addressed in several machines [1-6]. The technique is based on the stabilization of magnetohydrodynamic (MHD) modes through the localized injection of ECRH on a resonant surface [7]. So far, these experiments have dealt with L-mode plasmas and, with only the recent exception of ASDEX Upgrade [5], have been carried out in circular plasmas. A delay in the time of the disruption occurrence has been achieved in some cases and complete avoidance in other cases [1-6].

This paper reports on the first experiment of disruption avoidance with ECRH carried out in high performance H-mode plasmas. A scenario with high normalized pressure ($\beta_N = \beta(\%)/(I_p/aB_t)$ with β =ratio of volume averaged plasma pressure to magnetic field pressure, a =plasma minor radius, I_p =plasma current and B_t =toroidal magnetic field) has been set up in ASDEX Upgrade: $I_p=1$ MA, $B_t=2.1$ T, with NBI (~ 7.5 MW). In these discharges, at relatively low q_{95} and low density, neoclassical tearing modes (NTMs) are excited. NTMs are a major problem for any power generating fusion device (such as ITER) as, depending on the mode numbers, these pressure driven perturbations cause a degradation in confinement (with a mild reduction of the maximum achievable β_N) or can even lead to disruptions at low q_{95} . Disruptions occur when the modes eventually lock, i.e. when their rotation stops due to the interaction with the vessel wall or intrinsic error fields. The scheme of the disruption avoidance experiment in ASDEX Upgrade high β_N plasmas is the same successfully applied in previous similar experiments in FTU [5,6] and ASDEX Upgrade [5]. A reference

reproducible disruptive discharge is prepared: this discharge is then repeated with localized injection of ECRH triggered by a precursor signal (loop voltage (V_{loop}) and/or locked mode (LM)) via real-time control.

2. NTMs and high β_N disruptions

NTMs typically appear in discharges with high β_N . The flattening of the pressure profile over an existing magnetic island leads to a helical hole in the bootstrap current profile, which is the main drive for an NTM. The operational limit in plasma pressure (β -limit) at low q_{95} is often disruptive. Past experiments in ASDEX Upgrade [8] showed that an initial drop in β_N of typically 20% is due to the onset of a 3/2-NTM. When an additional 2/1 mode develops, the β -limit leads to a disruption: this usually occurs for $q_{95} \leq 3$ with $\beta_{N,max}$ ranging from 2 to 2.7. For $q_{95} > 3$, a non-disruptive soft β -limit by a 3/2-NTM is found ($\beta_{N,max} = 2.9$), sometimes followed by a further reduction of β_N to $\sim 0.7-0.8\beta_{N,max}$ due to a 2/1-NTM, depending on local stability parameters at the resonant surfaces. In this phase additional $n=1$ modes, dominated by the 2/1-NTM, appear (with coupling between 3/1, 2/1 and 1/1) and the discharge survives with a reduced confinement time. For intermediate to high q_{95} even a mode locking does not necessarily lead to a disruption. In this latter case a local stationary or modulated current drive with ECCD at the resonant surface of the dominant NTM (3/2 or 2/1) is able to remove the NTM and partially recover the confinement of the discharge [9]. The combined local heating and current drive replaces the missing bootstrap current and removes the island again. Anyway, in these experiments the modes have been stabilized from a ‘‘saturated’’ condition, by changing the sign of the growth rate, which is about zero at the moment of power injection: the stabilization is achieved with ~ 1 MW for the (3/2)-NTM and ~ 1.4 MW for the (2/1)-NTM [9]. On the contrary, acting on a disruptive phase implies dealing with a positive growth rate that is increasing the island dimension. A difference in the required ECRH power can then be expected, due to the plasma non-stationary phase in which the power is injected. The timing of the process and the selection of effective precursors (such as V_{loop} and LM detector) are particularly crucial in the case of high β_N disruptions due to the fast mode growth.

3. Experiments

The reference disruption (without any ECRH injection) is shown in FIG.1 (top), compared to a case of full avoidance using off-axis ECRH (FIG.1 (bottom)). The scenario is an H-mode plasma with $I_p=1$ MA and $B_t=2.1$ T; the line-averaged electron density is $\sim 5 \times 10^{19} \text{ m}^{-3}$. The additional power (NBI only) is stepped on during the plasma current ramp-up and ~ 7.5 MW are reached at 1.2 s; two of the beams are depositing at an off-axis position to achieve maximum performance. A very high value of β_N is reached in this phase ($\beta_N \sim 2.7$ with $q_{95} \sim 3.6$) and NTM modes ($m/n=3/2$ and 2/1) are clearly visible in the spectrogram from Mirnov signals (FIG.2). The 2/1 mode, which is rotating at a frequency of about 12 kHz at $t=1.3$ s, quickly grows in amplitude. During this phase this mode slightly moves inwards and its frequency decreases; it finally locks at ~ 1.38 s, when the 2/1 island has reached a width of about 12 cm (as deduced from ECE profile measurements, see FIG.3 (left)). In correspondence of the mode locking, there is a crash of the T_e profile ($t=1.386$ s): the temperature collapses to a flat profile (~ 0.4 keV) in a wide region between $R=1.82$ m and $R=2.06$ m (FIG.3 (left)). After the T_e crash, the discharge survives just for ~ 15 ms before the disruption current decay begins (at $t=1.400$ s (see FIG.3 (right))). The magnetic axis is at

$R_{axis} \sim 1.72$ m; note that the ECE measurements are carried out in the low field side (LFS) region.

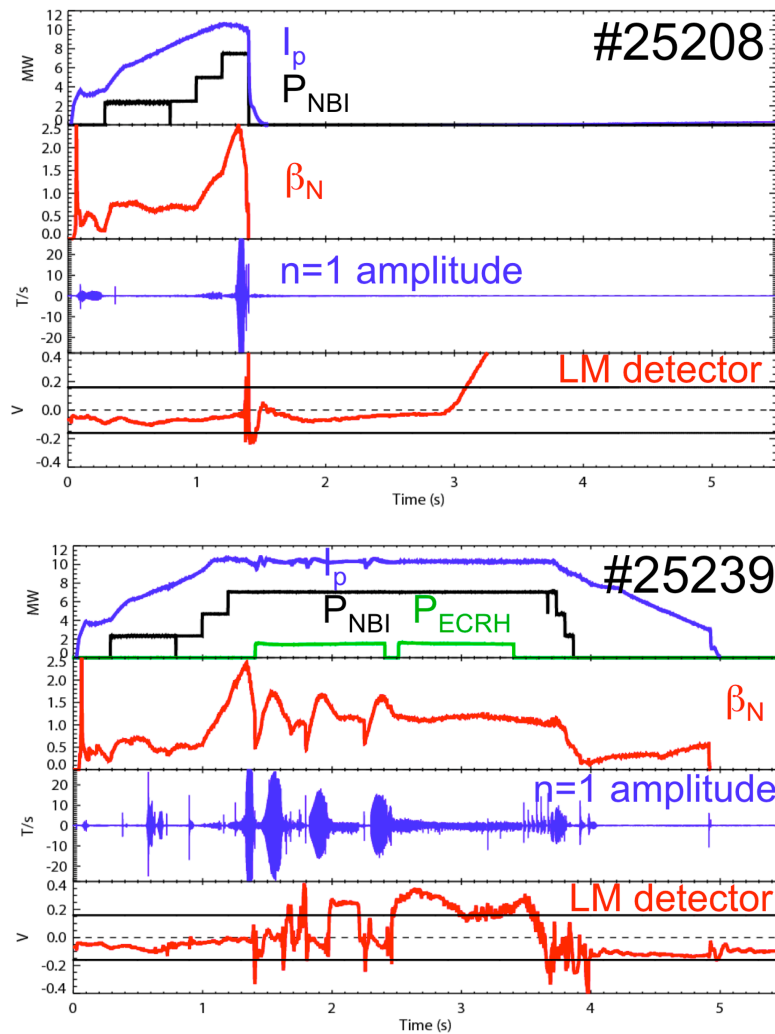


FIG. 1. (top) Reference disruption at high β_N : time traces of I_p , P_{NBI} , P_{ECRH} , β_N , Mirnov coil signal and locked mode (LM) detector signal with its thresholds. (bottom) Same discharge repeated with injection of ECRH ($\rho_{dep} \sim 0.5$) real-time triggered by LM.

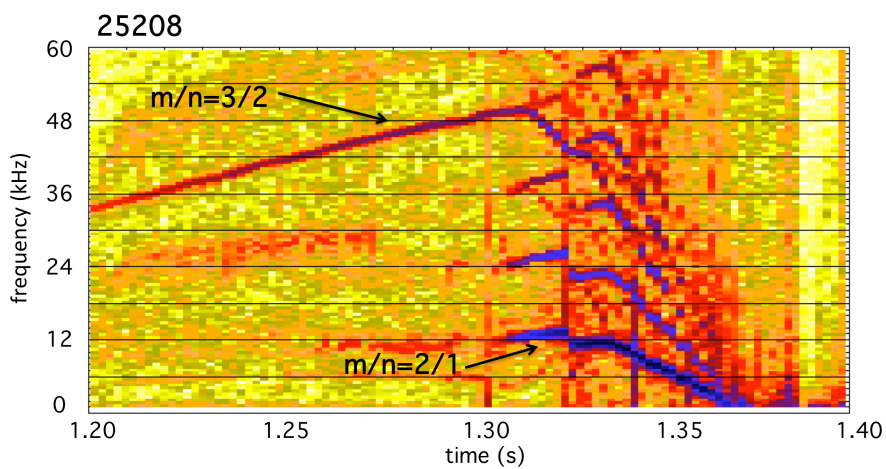


FIG. 2. Spectrogram from Mirnov coils data (dB_p/dt) for discharge 25208. The 3/2 and 2/1-NTM are indicated.

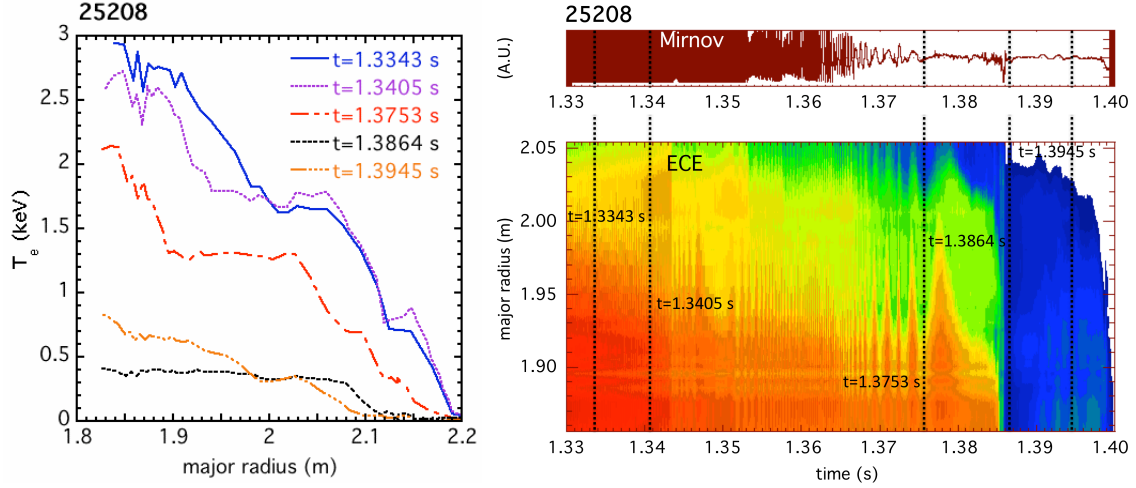


FIG. 3. Discharge 25208 prior to disruption: (left) ECE T_e profile evolution (times chosen to show profiles through island O-point); (right) ECE contour plot and Mirnov signal: the 2/1 island is slowing down until the locking and T_e crash at 1.386 s; the island is asymmetric (see for example at $t=1.3864$ s) and prior to the crash is centered at $R\sim 1.97$ m.

This disruption phenomenology confirms earlier ASDEX Upgrade experiments [8], but it is now found that the β -limit is disruptive even for $q_{95}>3$: this is probably linked to the lower density than in the past ($\sim 5\times 10^{19}$ m $^{-3}$ compared to $\sim 7.8\times 10^{19}$ m $^{-3}$).

The reference disruptive discharge has been used as a target for disruption avoidance experiments with ECRH application. Different ECRH launching angles have been set in different discharges. The poloidal launching angles of the mirrors (θ) have been varied so that in each discharge the power has been deposited onto a different poloidal (ρ_{dep}) and hence radial location. The target toroidal launching angle (φ) has been set to zero (*pure heating*) except for one discharge (#25255) in which the target φ has been set to -5° corresponding to a co-current drive (*co-ECCD*) configuration, resulting in the innermost deposition location of the whole scan. The old ASDEX Upgrade gyrotron system has been used: it consists of four gyrotrons (140 GHz) delivering a maximum of 0.4 MW each. The maximum total ECRH power injected in these discharges is ~ 1.5 MW. The second harmonic X-mode resonance (2.5 T) is on the high field side (HFS). Due to a technical failure, φ was always mechanically blocked to -10° for gyrotron 3, therefore providing a non-zero fraction of driven co-current.

A combination of LM monitor and V_{loop} signals has been used for the real-time triggering of ECRH: once above a preset threshold value, both signals can trigger independently the gyrotrons. In practice, the LM signal was found to be always the first one to trigger. The LM signal is generated from the difference of two saddle coils on the high field side with a toroidal distance of 180° . Each coil spans a toroidal angle of 180° and 20 cm in the poloidal direction. The ECRH pulse duration is set to 500 ms and the system can be re-triggered (this feature has been used in several discharges, for example in the one shown in FIG.1 (bottom)). ECRH is injected just after the locking of the 2/1 mode, when the electron temperature flattens to a low level. The poloidal angle scan roughly covers the range $\rho_{dep}=0.4-0.8$ as shown by the calculated ECRH power deposition profiles (FIG.4). The calculations have been performed, based on experimental electron density and temperature profiles, using both the ECWGB 3D quasi-optical ray tracing code [10] and TORBEAM [11] with similar results. Note the difference of just few centimeters in major radius between the various deposition locations in FIG.4 (left).

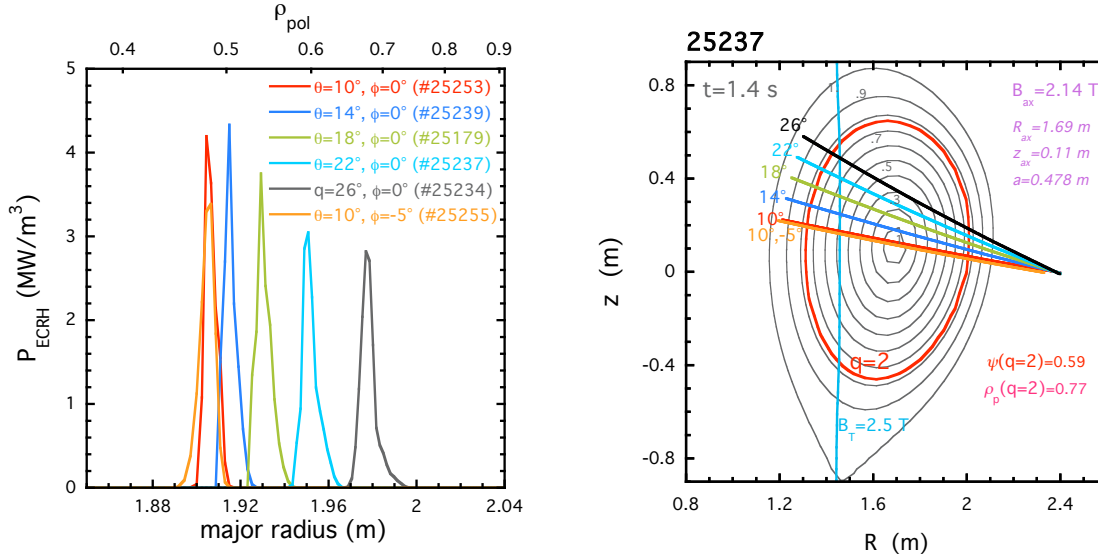


FIG. 4. (left) Comparison of typical ECRH power deposition profiles (from ECWGB 3D) obtained in the radial deposition scan. These profiles have been calculated using the experimental data of discharge #25237 at $t=1.4$ s. This time is representative of the discharge evolution after the 2/1 mode locking. The discharge numbers corresponding to each couple of launching angle settings (θ and ϕ) are also indicated. Gyrotron 3 power is not shown. (right) Equilibrium plot with ρ_{pol} contours (#25237, $t=1.4$ s).

A close look at the events occurring after the mode locking phase can be given in FIG.5 (left). β_N decreases due to the growing mode, which finally locks; ECRH is applied: soon after this the mode unlocks and, driven by the increasing β_N , grows again until a new maximum island width is reached. The effect of ECRH appears to be twofold: 1) to provide some heating to sustain the discharge; 2) to control the further evolution of the 2/1 mode. In order to compare the effectiveness of ECRH in different discharges we will consider the time delay between the initial locking of the 2/1 mode (t_{lock}) and the first maximum reached by the mode after ECRH application (t_{MHD}). This parameter can give a qualitative indication on how well ECRH manages to act on the MHD mode stabilization. A plot of $\Delta t = t_{\text{MHD}} - t_{\text{lock}}$ as a function of the poloidal launching angle is shown in FIG.5 (right).

The possibility of obtaining disruption avoidance depends upon the stabilizing effect of ECRH on the 2/1 mode and, therefore, in practice on the relative distance between the position of the island and the deposition location. When the ECRH deposition location exactly matches the position of the 2/1 mode or the power is deposited close to the $q=2$ surface (so that some power flows to the island anyway, at least for some time) this mode does not grow in amplitude or is partly stabilized and the discharge can fully recover (#25179, #25253, #25237, #25239). When the deposition location is well off the 2/1 location, the mode is not controlled and the discharge disrupts essentially as in the reference discharge (#25255, #25234). By repeating discharge #25253 with half ECRH injected power (#25256) no disruption avoidance has been obtained.

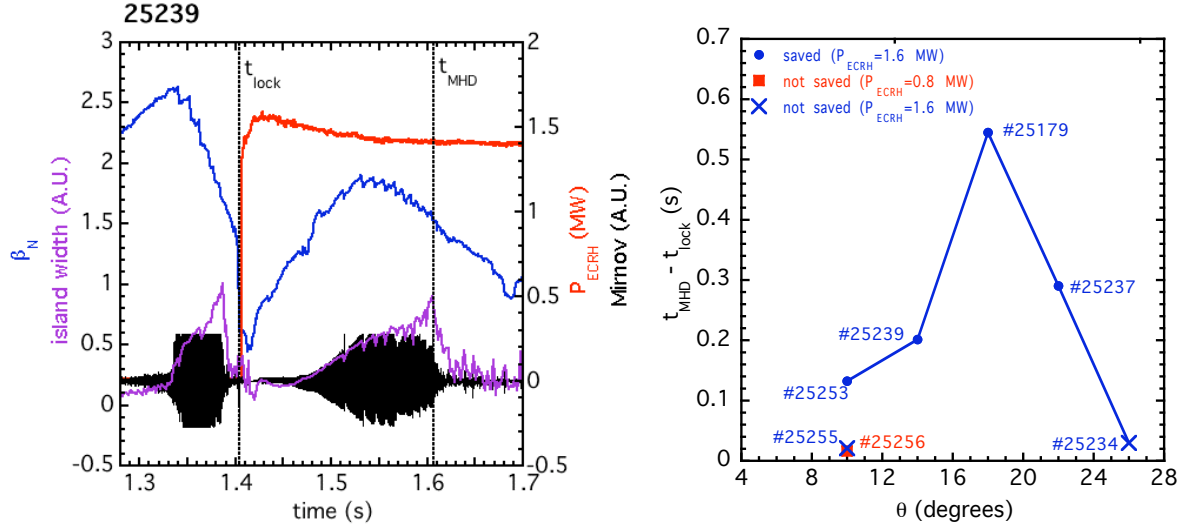


FIG. 5. (left) Zoom in the time interval when ECRH is applied (discharge 25239): the time traces of β_N , estimated width of the 2/1 island (from Mirnov), P_{ECRH} and Mirnov coil signal are shown. (right) Difference between the time of maximum amplitude of the 2/1 mode after the T_e crash (t_{MHD}) and the time of mode locking (t_{lock}) plotted as a function of the poloidal ECRH launching angle of each discharge.

4. Analysis of the island evolution

A generalized Rutherford equation (including asymmetric island parameters) describing the mode amplitude and frequency evolution [12] has been used to analyze the island evolution and to confirm the qualitative picture described in the previous Section. Both ECE T_e and CXRS T_i profiles have been employed in the determination of the pressure profiles used in the analysis. From the observation of ECE contour profiles it can be seen that the islands are radially asymmetric [13], with a larger extension of the side of the island closer to the plasma axis (see FIG.3 (right)).

The results of the simulation are presented for three discharges in FIG.6 (a),(b),(c). The time evolution of the experimental island width is derived from the inspection of the ECE T_e profiles. This implies an underestimate of the actual width during the phases in which the mode is locked (indicated by shaded areas in FIG.6). The modelled island width is obtained from the solution of the generalized Rutherford equation. The evolution of the island prior to the T_e crash (no ECRH in this phase) is found to be well described in all cases. In the second phase, after the T_e crash, the fraction of ECRH power absorbed in the island has been used as a free parameter in order to reproduce the time evolution of the experimental island widths for each discharge. It is found that the best matching between model and experimental data is obtained with an ECRH absorbed fraction of $\sim 56\%$, $\sim 53\%$ and $\sim 31\%$, respectively for discharges #25179, #25237 and #25253. FIG.6(d) shows an example of the level of overlapping between the ranges of the measured island location and calculated power deposition location (discharge #25253). The above fractions of ECRH power absorbed in the island are time-averaged values: in reality, as the relative positions of the island and the injected power vary in time (FIG.6 (d)) the level of deposited power is also expected to change accordingly. The Rutherford equation analysis therefore suggests that in these discharges the deposition location has been set quite close to the $q=2$ surface, in agreement with the qualitative findings presented in FIG.5 (right).

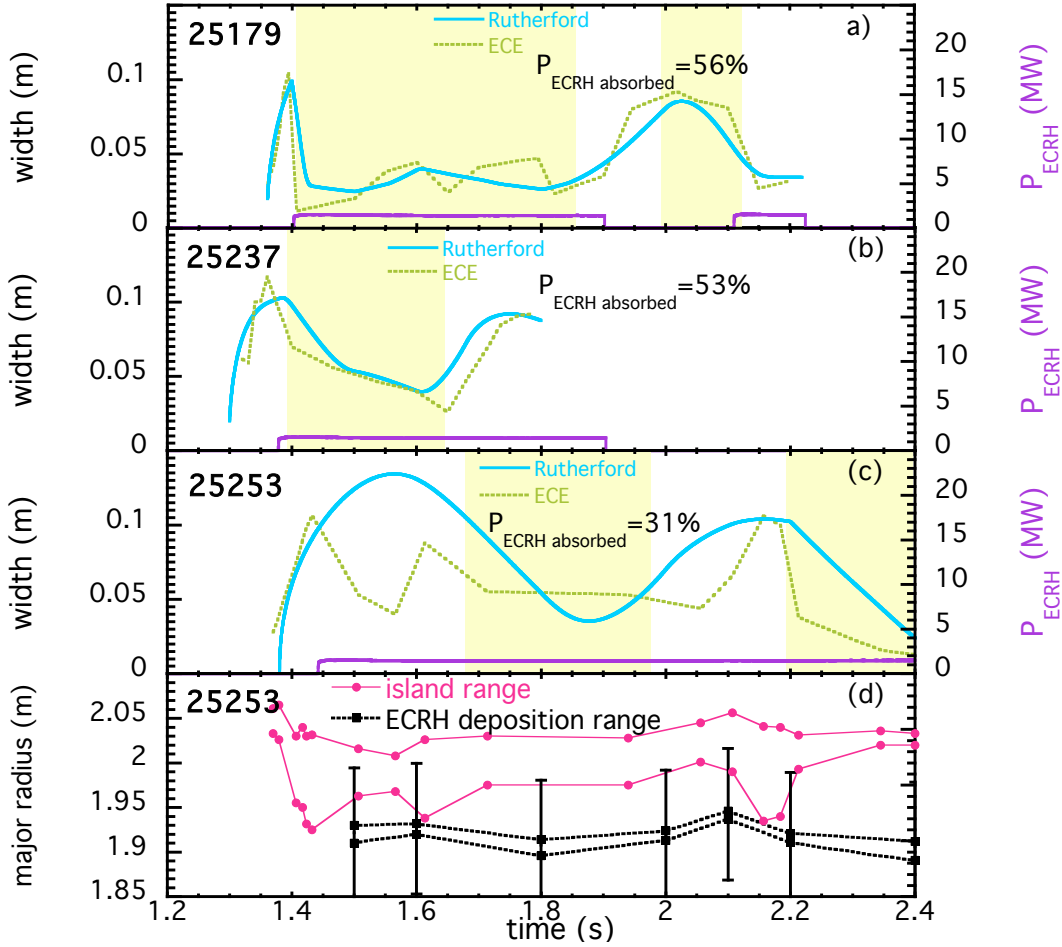


FIG. 6. (a), (b) and (c) Rutherford equation analysis respectively for discharges #25179 (ECRH launching angles: $\theta=18^\circ$, $\phi=0^\circ$), #25237 ($\theta=22^\circ$, $\phi=0^\circ$) and #25253 ($\theta=10^\circ$, $\phi=0^\circ$); yellow shaded areas indicate the time slices in which the mode is seen to be locked. (d) Discharge #25253: comparison between the 2/1 island location (from ECE) and the calculated ECRH deposition radius (with $\pm 3.5\%$ error bars to account for equilibrium reconstruction uncertainty).

5. Conclusions

The localized injection of ECRH has been investigated as a tool for disruption avoidance in high β_N H-mode plasmas in ASDEX Upgrade. Disruption avoidance has been obtained reproducibly by means of localized injection of 1.5 MW of ECRH in a target plasma with ~ 7.5 MW of total power, corresponding to only $\sim 20\%$ additional ECRH power. The observations indicate that injection close to the $q=2$ surface enables the control of the $m/n=2/1$ mode therefore leading to disruption avoidance. Moreover, even if the discharge may not fully be recovered, a disruption delay can be obtained, thus opening the way for further possible discharge shutdown measures. These results indicate that ECRH injection can be considered as an alternative technique to massive gas injection for active disruption control through avoidance (and a consequent controlled current termination procedure) instead of mitigation of dangerous effects.

Further experiments on avoidance of disruptions at high β_N should address the following issues: a) determination of the ECRH power threshold; b) evaluation of the effect of the timing of ECRH; c) comparison of ECRH and ECCD. Long-term work may include the extension of these techniques to other types of disruptions in H-mode (e.g.: due to impurity injection) and to the use of a real time tracking of the resonant surface.

References

- [1] HOSHINO, K., et al., “Avoidance of $q_a=3$ Disruption by Electron Cyclotron Heating in the JFT-2M Tokamak”, *Phys. Rev. Lett.* **69** (1992) 2208.
- [2] KISLOV, D.A., et al., “The $m = 2, n = 1$ Mode Suppression by ECRH on the T-10 Tokamak”, *Nucl. Fusion* **37** (1997) 339.
- [3] SAVRUKHIN, P.V., et al., “Coupling of internal $m = 1$ and $m = 2$ modes at density limit disruptions in the T-10 Tokamak”, *Nucl. Fusion* **34** (1994) 317.
- [4] SALZEDAS, F., et al., “The effect of ECRH on the stability of the radiation induced $m = 2$ mode and on the current quench of a major disruption”, *Nucl. Fusion* **42** (2002) 881.
- [5] ESPOSITO, B., et al., “Disruption control on FTU and ASDEX upgrade with ECRH”, *Nucl. Fusion* **49** (2009) 065014.
- [6] ESPOSITO, B., et al., “Disruption Avoidance in the Frascati Tokamak Upgrade by Means of Magnetohydrodynamic Mode Stabilization Using Electron-Cyclotron-Resonance Heating”, *Phys. Rev. Lett.* **100** (2008) 045006-1.
- [7] GIRUZZI, G., et al., “Dynamical modelling of tearing mode stabilization by RF current drive”, *Nucl. Fusion* **39** (1999) 107.
- [8] ZOHN, H., et al., “MHD stability and disruption physics in ASDEX Upgrade”, *Plasma Phys. Control. Fusion* **37** (1995) A313.
- [9] MARASCHEK, M., et al., “Active control of MHD instabilities by ECCD in ASDEX Upgrade”, *Nucl. Fusion* **45** (2005) 1369.
- [10] NOWAK, S. and OREFICE, A., “Three-dimensional propagation and absorption of high frequency Gaussian beams in magnetoactive plasmas”, *Phys. Plasmas* **1** (1994) 1242.
- [11] POLI, E., et al., “TORBEAM, a beam tracing code for electron-cyclotron waves in tokamak plasmas”, *Comput. Phys. Commun.* **136** (2001) 90.
- [12] LAZZARO, E. and NOWAK, S., “ECCD control of dynamics of asymmetric magnetic islands in a sheared flow”, *Plasma Phys. Control. Fusion* **51** (2009) 035005.
- [13] URSO, L., et al., “ASDEX Upgrade—JT-60U comparison and ECRH power requirements for NTM stabilization in ITER”, *Nucl. Fusion* **50** (2010) 025010.